STUDY ON DYNAMIC GROUND CHARACTERISTICS IN RANGE OF SHORT AND LONG PERIODS

by

Yoshikazu KITAGAWA[I] and Yutaka MATSUSHIMA[II]

SUMMARY

The dynamic characteristics of soil-layers in the wide range of periods are investigated, taking the Sendai district damaged by the Off-Miyagi Prefecture Earthquake (1978) as an example. The deep ground characters in long periods are estimated from the seismic data published by J. M. A. In order to estimate earthquake motions on the ground surface in short periods, strong motions observed in a building are analyzed with consideration of building-subsoil intraction to get the incident wave at the structural base rock. The comparison of microzoming maps with real damages to buildings is carried out. The close correlation between the both is recognized.

INTRODUCTION

It is one of the most important problems in the field of earthquake engineering to predict the maximum earthquake motions in a certain place which may be defined by the seismic activity and ground characteristics. In order to clarify this more reliably, it is necessary to investigate separately each of them. Generally the ground motion in the frequency domain (G(jw)) will by expressed by the following equation,

$$G(jw) = (FS(jw) \cdot TF(jw)) \cdot ST(jw), \qquad \text{---------- (1)}$$

where FS(jw), TF(jw) and ST(jw) represent the spectrum of the focal mechanism, the overall transmission function for the generation and propagation of earthquake waves, and the function for the wave propagation of local soil layers, respectively. The former part in parentheses of the equation stands for the theoretical seismic records based on the focal mechanism, and the latter for the ground motion dealt with in the earthquake engineering.

It is pointed out that the long period ($10 \geqq T > 1.0$ sec.) cerresponding to the ground characteristics of fairly large area is amplified by soil layers with the depth varying from a few hundred meters to 1~2 kilometers and that the short period ($T \leqq 1.0$ sec.) corresporting to the ground characteristics just beneath a construction is affected by soil-layers with the depth less than a few hundred meters. The former corresponds to the seismic macrozoning and the latter to the seismic microzoning. According to those two categories, the seismic base rock with the shear wave velocity of 2~3 km/sec. and the structural base rock with the shear wave velocity of 700 m/sec. are set up.

I. Head of Structure Div., Building Research Institute, Min. of Const., Japanese Government

II. Head of Dynamics Div., Building Research Institute, Min. of Const., Japanese Government

The estimation of ground characteristics in the range of short periods is performed based on the results of the analytical investigation of the elastic system with damping which is independent of frequency as well as of microtremor measurements. The various seismic microzoning maps thus obtained are compared with the distribution of real damages to buildings.

OUTLINE OF GEOLOGICAL CONDITION

Topographical Aspects— As for the geological conditions of surface soil, the Sendai district is generally classified into three areas as shown in Fig. 1. ; (1) the hilly tertiary terrain, (2) the terrace area and (3) the alluvial plain. The oblique NE-SW line passing near the center of the map is called the Rifu-Nagamachi techtonic line. The area in the west of the tectonic line is characterized by the hilly tertiary terrain and the several levels of the terraces. The surface deposit of this terrace is loam which is underlain by hard clay, gravels, pelite and shale. The hilly terrain is either of very hard andesite and shale, but the surface is covered with loam at several places. The alluvial plain develops in the east of this line and is mostly of sand, silt and gravels.

The depth of the tertiary base rock varies abruptly near the tectonic line. There are several areas in the plain which are covered by very soft peat or mud. The soil profile and the results of seismic prospecting tests by the well shooting method at representative places in the terrace area and the alluvial area are shown in Fig. 2.

Microtremor Measurements— The microtremors are measured at several sites shown in Fig. 1 with electromagnetic seismometer having the natural period of 1.0 sec. to get dynamic properties of soil-layers.[1] The area where the measurements were performed belongs to two types of geological conditions (2) and (3) mentioned above. The representative Fourier spectra of microtremors in NS and EW directions are shown in Fig. 3, where sites G-06 through G-08 and sites G-17 and G-18 are on the outcrop of terrace and on the alluvial plain, respectively. The peaks at long periods more than 1.0 sec. reflect the deep ground characteristics, whereas the peaks at short periods less than 1.0 sec. do the shallow ground ones.

Quake Degree for Deep Ground Structure— The values of the maximum displacements of NS and EW components (A_{NS} and A_{EW}, micron) observed at various stations of Japanese Meteorological Agency are substituted in the Tsuboi's formula to get the magnitude (M) of the earthquake as the average. Under the assumption that 10^{β} is always regarded as the standard amplitude in the range of the long period reflecting the deep ground characteristics of a fairly large area, the following value is calculated at the J. M. A. station in the Sendai district;

$$F = \frac{1}{m} \sum_{i=1}^{m} \left(\sqrt{A_{NS}^2(T_i) + A_{EW}^2(T_i)} \right) / 10^{\beta} , \qquad \text{---------- (2)}$$

where $\beta = M - 1.73 \log\Delta + 0.83$. Δ, T_i and m denote the epicentral distance (km), the period of the phases giving the maximum displacement amplitude and the total number of the earthquake data, respectively.[2] Consequently the value of F means the averaged amplitude at the Sendai station normalized by the standard one. Figs. 4 and 5 show the F value caluculated by Eq. (2) and the number of data, respectively. It is found that the degree of the quake relative to the standard one is high at the periods of 3.0 and 5.0 sec.

and that the number of data is great at the periods of 1.0 and 2.0 sec.

Setting up of Structural Base Rock— The transfer function, which is defined by the ratio of the wave on the ground surface (Uo) to the incident wave (Uin), for the deep underground structure and for the shallow one at a representative place in the terrace near the Sendai station of J. M. A. are shown in Fig. 6. The shear wave velocities V and densities ρ of the various soil-layers were determined by the seismic prospecting test, the seismic data of strong motion seismographs of J. M. A. and the boring tests. As seen in Fig. 6, there are some peaks depending on the levels of the base rock but the predominaut frequency between 3.0 and 4.0 Hz is common to the both. This frequency also appears in the results obtained by microtremor measurments at the sites G-06 through G-08.

Consequently in this study, the structural base rock with shear wave velocity of 700 m/sec is set up to get the ground characteristics in the range of short periods less than 1.0 sec. The values of shear wave velocity at intervals of 0.5' in both Latitude and Longitude in the Sendai district are estimated from the soil profile, results of the penetration tests and the geolocical conditions. Fig. 7 displays, as an example, the profile of shear wave velocity on A-A' section (line of N38°15'30") indicated in Fig. 1.

SEISMIC MICROZONING

Incident Wave Motions in the Structural Base Rock— In order to estimate the earthquake motions on the ground surface, the strong motions observed at the Sendai Sumitomo Building[3] during the Off-Miyagi Prefecture Earthquake of June, 1978 (M=7.4) were analyzed with consideration of building-subsoil interaction to get the incident wave at the structural base rock with shear wave velocity of 700 m/sec. This is an eighteen-storied steel framed reinforced concrete structure with two-storied basements. The plan and elevation of this building are shown in Fig. 8, where the locations of strong motion accelerographs are indicated. Fig. 9 shows the accelerograms recorded at the 2nd basement floor. Fig. 10 displays the Fourier spectra for the accelerograms at the 18th floor and the 2nd basement floor together with the spectral ratios between the both.

The building and subsoil were idealized as an elastic one-dimensional continuous media with some amount of damping which is independent of frequency. The parameters required in the analysis were determined based on the results of these Fourier spectral ratios and seismic prospecting. The rigidities and densities for the layers representing the building and the first soil layer were modified so as to approximately satisfy the compatibility at the boundary, assuming that shear waves are propagated and reflected only in the vertical direction.[4] Fig. 11 shows the observed and the culculated maximum accelerations in NS and EW directions together with the assumed shear wave velocities of this particular site. Fig. 12 indicates the response acceleration spectra with damping ratio (h) of 0.05 for the observed wave at the 2nd basement floor, the calculated incident wave at structural base rock, and the calculated wave at outcropping of the 2nd basement floor level in NS and EW directions.

Using those two components at the base rock, a wave form for the major principal axis[5] was calculated, which was taken as the final incident wave. The direction of its axis was N18.5°E in two-dimensional space. Fig. 13 shows the resultant incident wave motion at the structural base rock.

Distribution of Dynamic Characteristics for Underground Structure— The predominant period and the magnification factor are caluculated at intervals of 0.5' in both Latitude and Longitude by the Haskell's Method. The distribution maps for the predominant period and the magnification factor of the underground structure above the structural base rock are shown in Figs. 14 and 15, respectively. As found from these figures, the predominant periods are around 0.2~0.3 sec. in the terrace area and 0.3~0.8 sec. in the alluvial plain. Similarly the magnification factors are about 2~3 in the former and 3~5 in the latter.

Distribution of Maximum Acceleration and Velocity— The maximum acceleration and velocity on the ground surface are calculated as the response due to the aforementioned incident wave on the structural base rock. The distribution maps of maximum acceleration and velocity are illustrated in Figs. 16 and 17, where the values of contour lines are normalized by the maximum value of those maxima. As seen in these figures, the value in the alluvial plain is about 1.5 times as much as that of the several levels of the terraces.

Distribution of Ductility Factor— The responses of inelastic sigle-degree-of-freedom systems having degrading bilinear hysteresis when subjected to the motions on the ground surface are evaluated. The distribution maps of the ductility factor for the supper-structure, which is defined by the absolute maximum displacement normalized by the yield displacement, with the damping ratio (h) of 0.05 and the yielding base shear coefficient of 0.3 are shown in Figs. 18 (a) ~ (c), where typical values are selected for the periods of the system in an elastic range. As is recognized from these figures, the distribution pattern is not sensitive to the natural periods of super-structures. As a rule, contour lines of ductility factors for shorter periods is similar to those of the maximum accelerations. As the period increases, these look like those of the maximum velocities.

COMPARISON OF DAMAGES TO STRUCTURES WITH MICROZONING MAPS

Extents of Damages to Buildings— Fig. 19 shows the distribution of damages to reinforced concrete buildings, steel buildings, wooden houses and landslide areas in the Sendai district. The severe damages to reinforced concrete and to steel structures were concentrated on the deluvium and on the alluvial plain respectively. Damages to wooden houses were on the alluvium and on the several levels of terrace.

Three-storied reinforced concrete buildings were exhaustively damaged by shear failure of columns in the first story. Almost all of damages to low-rise steel structures were brought about by buckling and breaking of bracings and failure of anchoring. The damages to wooden houses can be classified into two types; (1) damages due to ground motions on the alluvium plain and (2) damages due to landslide of embankment on the terrace.

Comparison of Distribution of Damage with Zoning Maps— From the comparison of Fig. 19 with Fig. 16 or Fig. 18, the close correlation between the location of severely damaged structures and the distribution of the maximum acceleration or of the ductility factor is generally recognized. It should be noted, however, that the soil is assumed to behave elastically in the foregoing analyses. In the case of severe earthquakes, this will be the crude approximation and should be modified. In this sense, underground structures

have been modelled by the hysteretic nonlinear systems although reliable values about the nonlinearity of soil in this district are not available. Fig. 20 illustrates an example which gives the distribution of maximum accelerations obtained by such inelastic analysis where the Ramberg-Osgood hysteresis is assumed for the restoring force characteristics of soil deposits.[6] It seems that the maximum accelerations tend to distribute more uniformly than those in Fig. 16. The more detailed and parametric nonlinear analysis will be needed for the future study.

CONCLUDING REMARKS

The dynamic characteristics of underground- and super-structures in the Sendai district are investigated. The deep ground characters are estimated by the data of strong motion seismographs of J. M. A. The shallow ground characters are evaluated by the microtremor measurements, boring data, penetration tests and so on. The incident wave motion is calculated by the aid of strong motion accelerograms recorded during the Off-Miyagi Prefecture Earthquake. The predominant periods, magnification factors, maximum accelerations and velocities on the ground surface and the ductility factors of super-structures are computed. The real damages to buildings are compared with such microzoning maps. The close correlation between the both is recognized. As the results, it is pointed out that the analytical investigation presented herein is appropriate for the seismic microzoning maps.

ACKNOWLEDGMENTS

The authors would like to acknowledge the continuing encouragement of Dr. M. Watabe, Director of Structural Dept.,Building Research Institute. In preparing the present paper, Mr. M. Tohdo, Res. Memb. of Toda Const. Co. Ltd., contributed a great deal. The authors also wish to express their sincere thanks to Dr. Y. Sugimura, Head of Geotechical Eng. Div., B. R. I., for his help with a large amount of geological data; and to Mr. T. Kashima and Miss M. Makishima, Membs. of B. R. I., for drawing figures and typing a manuscript. This work was partially supported by the finance provided by Science and Technology Agency.

REFERENCES

1) "Report on the Damage by 1978 Off Miyagi Prefecture Earthquake (in Japanese)", Rept. of B. R. I., No.86, PP.57-81, 1979.

2) Y. KITAGAWA and M. OZAKI ; "Study on Regional Characteristics of Maximum Earthquake Motion in Japan", Proc. of 5-th J. E. E., PP.1-8, 1978.

3) "Report on the Damage by 1978 Off-Miyagi Prefecture Earthquake (in Japanese)", Rept. of S. T. A., No.15, PP.58-60, 1978.

4) Y. OSAWA, Y. KITAGAWA and K. ISHIDA ; "Response Analyses of Earthquake Motions Observed in and around a Reinforced Concrete Building Including Building-Subsoil System", Proc. of 5-th W. C. E. E., 1973.

5) J. PENZIEN and M. WATABE, "Characteristics of 3- Dimensional Earthquake Ground Motions", Earthq. Eng. Struct. Dyn. 3, PP.365-373, 1975.

6) Y. OHSAKI, A. HARA and Y. KIYOTA ; Stress-Strain Model of Soils for Seismic Analysis (in Japanese)", Proc. of 5-th J. E. E, PP.679-704, 1978.

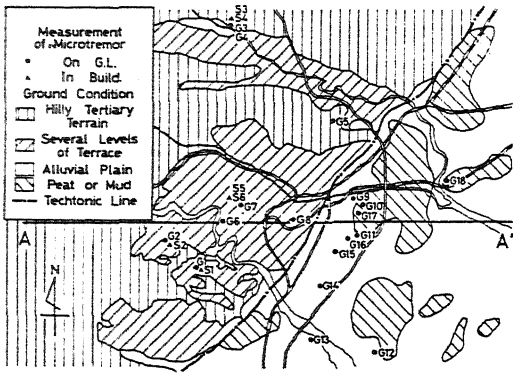

Fig.1 Geological Condition

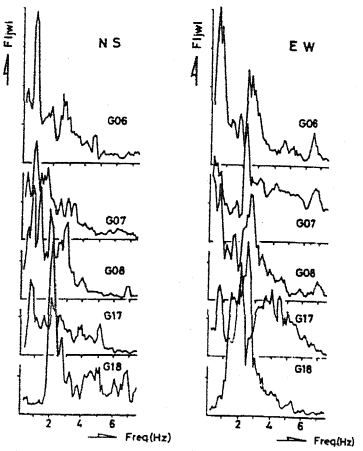

Fig.3 Fourier Spectra

GL	Name	V (m/s)	ρ (t/m³)	H (m)	Q
0	Loam	120	1.6	2	10
	Gravel	300	1.8	3	15
	Clay				
10	Petite	400	1.8	7	20
20	Pelite	500	1.9	25	30
30					
40	Shale	700	2.0	∞	50

GL	Name	V (m/s)	ρ (t/m³)	H (m)	Q
0	Peat	80	1.6	2	8
	Gravel	280	1.8	3	10
10					
20	Gravel	510	1.9	32	30
30					
40	Shale	700	2.0	∞	50

Fig.2 Profile of Subsoil

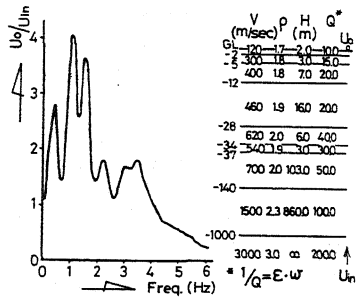

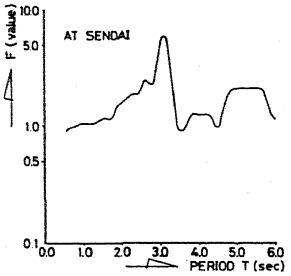

Fig.4 F-Value

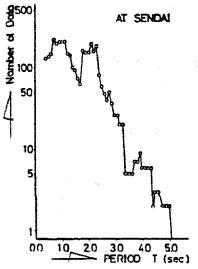

Fig.5 Number of Data

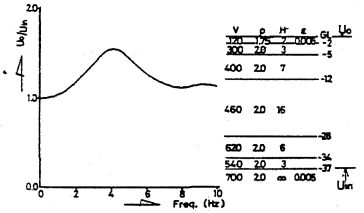

Fig.6 Transfer Function

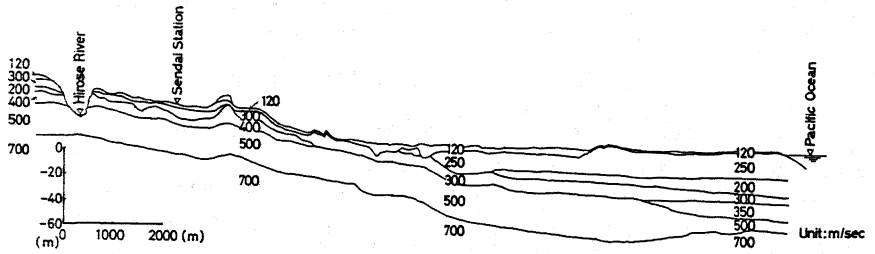

Fig.7 Profile of Shear Wave Velocity (A-A' Section)

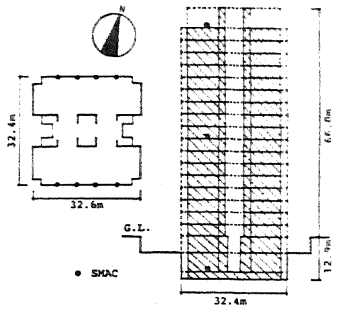

Fig.8 Plan and Section

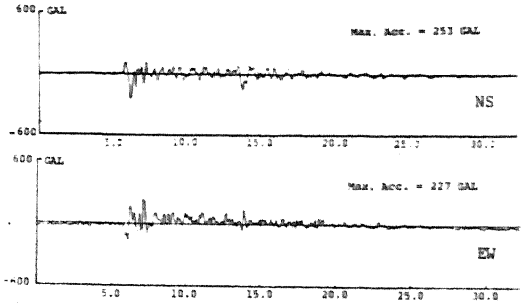

Fig.9 Accelerograms at 2nd Basement Floor

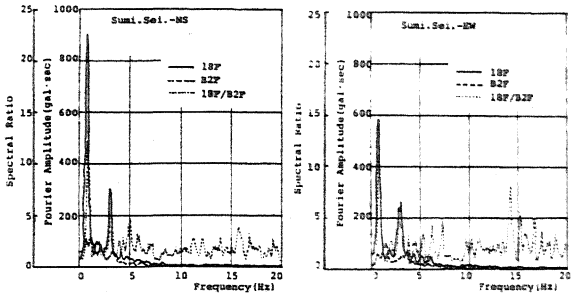

Fig.10 Fourier Spectra and Spectral Ratio

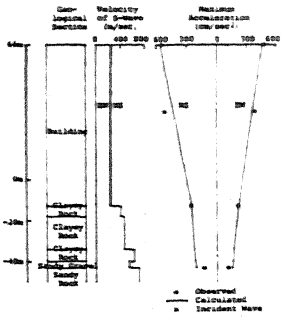

Fig.11 Max. Acceleration Values

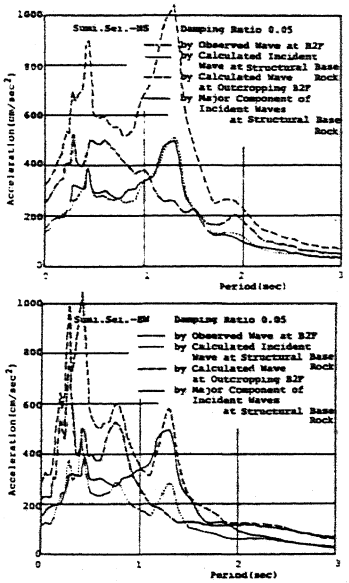

Fig.12 Response Spectra

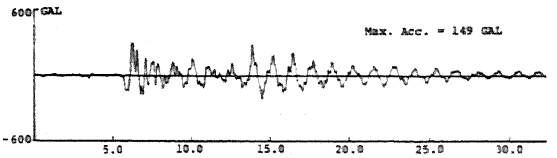

Fig.13 Final Incident Wave

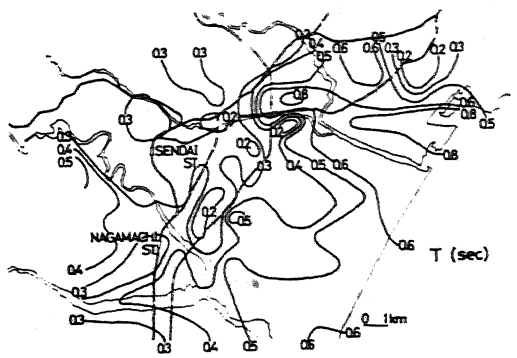

Fig.14 Distribution Map of Predominant Period

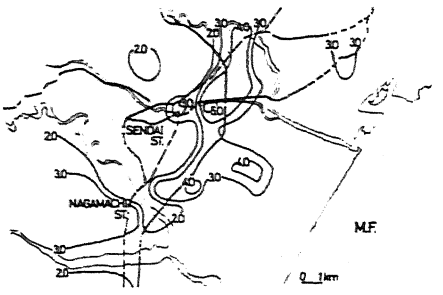

Fig.15 Distribution Map of Magnification Factor

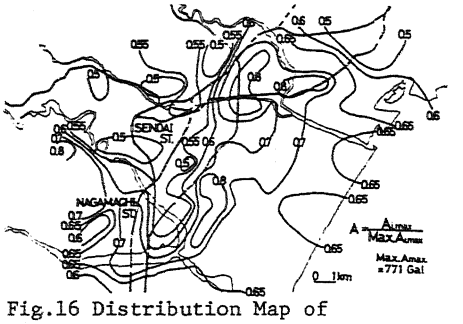

Fig.16 Distribution Map of Max. Acceleration

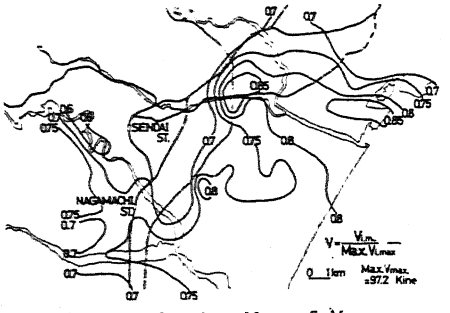

Fig.17 Distribution Map of Max. Velocity

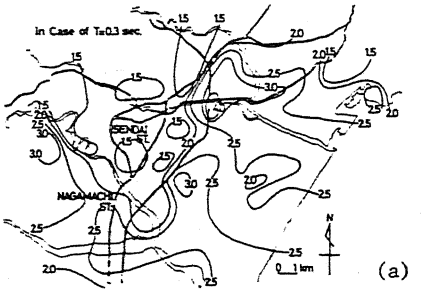

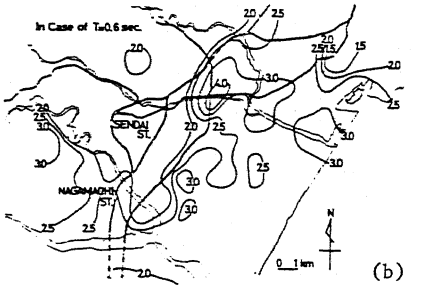

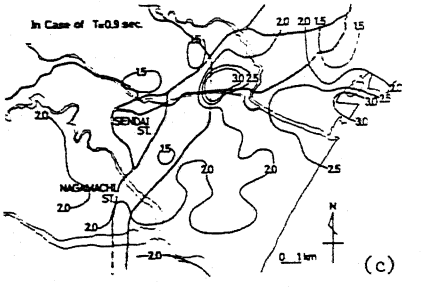

Fig.18 Distribution Map of Ductility Factor

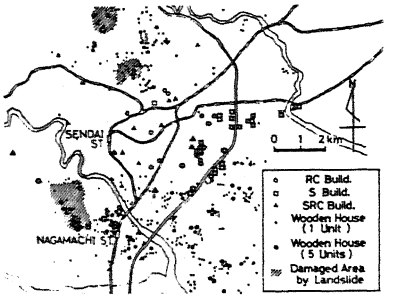

Fig.19 Distribution Map of Damages

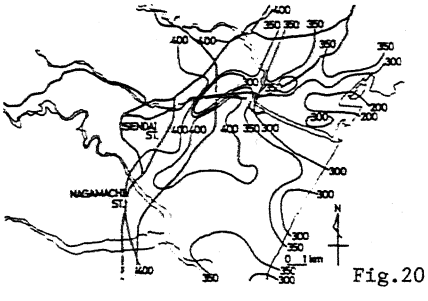

Fig.20 Distribution Map of Max. Acceleration